CHEMISTRY OF MATERIALS

ARTICLE

pubs.acs.org/cm

Plasma-Enhanced Atomic Layer Deposition of Silver Thin Films

Maarit Kariniemi,*[,†] Jaakko Niinistö,[†] Timo Hatanpää,[†] Marianna Kemell,[†] Timo Sajavaara,[‡] Mikko Ritala,[†] and Markku Leskelä[†]

[†]Laboratory of Inorganic Chemistry, University of Helsinki, P.O. Box 55, FI-00014 University of Helsinki, Finland

[‡]Department of Physics, University of Jyväskylä, P.O. Box 35, FI-40014 University of Jyväskylä, Finland

Supporting Information

ABSTRACT: Thermal properties of various silver precursors known in the literature were evaluated in order to discover which precursor is the most suitable one for plasma-enhanced atomic layer deposition (PEALD) of silver thin films. Ag(fod)(PEt_3) (fod = 2,2-dimethyl-6,6,7,7,8,8,8-heptafluorooctane-3,5-dionato) was found to be the best choice. Using Ag(fod)(PEt_3) together with plasma-activated hydrogen, silver thin films were deposited at growth temperatures of 120−150 °C, and ALD-type saturative growth was achieved at 120−140 °C. At 120 °C, the growth rate was 0.03 nm per cycle. The plasma exposure time had also an effect on the growth rate: with shorter exposure times, the growth rate was lower over the whole deposition area. The films deposited at 120 °C contained relatively small amounts of impurities, but these still affected the electrical properties of the films. The resistivities were relatively low: about 20 nm thick films had a resistivity of 6−8 $\mu\Omega\cdot$cm. The morphology and the crystal structure of the films were analyzed as well.

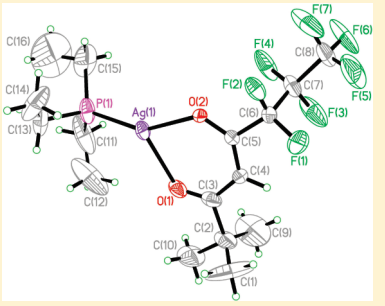

KEYWORDS: plasma-enhanced atomic layer deposition, silver β-diketonates, silver thin film, plasmonics

INTRODUCTION

Recently there has been growing interest toward conformal silver thin films deposited with atomic layer deposition (ALD) due to the possibile use of silver in plasmonic devices. ALD is a thin film deposition method capable of growing high-quality films with perfect conformality and thickness control.[1,2] In plasmonics, silver can be employed in harnessing surface plasmons. Surface plasmons can be generated at a metal/dielectric interface when the electromagnetic field of light interacts resonantly with the electrons near the surface of the metal.[3] The intensity of a plasmon is decaying because of losses arising from absorption in the metal, but silver has the lowest losses in the visible spectrum.[4] The propagation distance[3] and the intensity of the field can be affected by patterning the surface.[4] By patterning, one can tailor surface plasmons to specific applications. In general, surface plasmons can potentially be used in several applications such as optics, magneto-optic data storage, microscopy, and solar cells.[4] In optics, the generation of a surface plasmon makes it possible to, for example, concentrate light to a subwavelength optical structure. Without exploiting plasmons, the dimensions of optical components have to be larger than the wavelength of the light to avoid the obstruction of the light by diffraction.[3]

Silver has also the lowest resistivity of all known elements (1.59 $\mu\Omega\cdot$cm), which makes it an attractive material also for interconnects in microelectronics.[5] Other applications for silver films include highly reflective mirrors and decorative coatings. Silver is also a potential alternative for antimicrobial coatings.[6]

A common concern regarding thin films of silver is their limited chemical stability. Silver oxidizes in air and reacts with sulfur compounds in the atmosphere, leading to a contaminating adlayer of Ag_2S. The limited chemical stability can restrict the use of silver in some applications. However, if the instability is not an issue, silver is a rather inexpensive noble metal for various applications. The chemical reactions of a silver surface can be hindered by a barrier layer.[7]

Silver thin films have conventionally been prepared with different physical[8−10] and chemical vapor deposition (CVD) techniques.[11−14] However, when it comes to ALD, only in one previous study, silver thin films were deposited by remote plasma-enhanced atomic layer deposition (PEALD).[15] The self-limiting growth was verified only at a one temperature (∼140 °C) being limited by source temperature at the lower side and precursor decomposition at the higher side. In addition, considerable amounts of impurities were found in the films. The impurities were phosphorus (4.0 at.%), oxygen (10 at.%), hydrogen (5 at.%), and carbon (1 at.%). In spite of impurities, the electrical properties were relatively good: the resistivity of a 40 nm thick film was 6 $\mu\Omega\cdot$cm. It should also be noted that the silver thin films were grown on relatively small substrates (5 × 5 cm^2), and thus, there is certainly a need for large scale silver ALD processes. Recently, a report of silver nanoparticle deposition with liquid injection ALD was published, but it appears that this process does not allow the deposition of uniform continuous films.[16] The small number of ALD silver studies can be attributed to the lack of sufficiently stable and volatile precursors. Generally, in many other cases, the earlier established CVD precursors

Received: February 8, 2011
Revised: April 20, 2011
Published: May 10, 2011

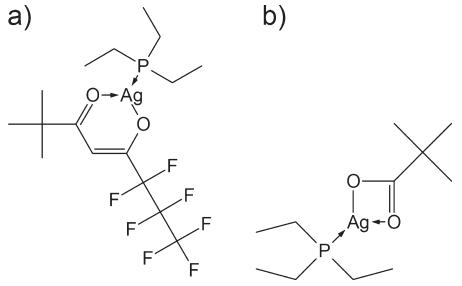

Figure 1. Molecular structures of (a) Ag(fod)(PEt_3) and (b) Ag(Piv)(PEt_3).

could have been utilized in ALD. However, in the case of silver, most of the sufficiently volatile CVD precursors have limited thermal stability. In the present investigation, the thermal properties of various silver compounds were evaluated to explore the possibility of using these precursors in an ALD process. It was found out that (2,2-dimethyl-6,6,7,7,8,8,8-heptafluorooctane-3,5-dionato)silver(I)-triethyl-phosphine (Ag(fod)(PEt_3))[11−14] is suitable for the deposition of silver thin films on large area substrates by PEALD using hydrogen plasma as a reducing agent.

In this article, we present a novel PEALD process for silver thin films. For the first time, silver thin films are being deposited with ALD in an industrial scale reactor up to 200 mm wafer sizes. The crystal structure, morphology, composition, and electrical properties of the deposited films are analyzed.

EXPERIMENTAL SECTION

Synthesis and Characterization of the Precursor Compounds. The synthesis and manipulation of the compounds were done under inert atmosphere or vacuum using standard Schlenk techniques and a glovebox.

Silver compounds Ag(fod), Ag(thd)(PEt_3) (thd = 2,2,6,6-tetramethylheptane-3,5-dionato), Ag(fod)(PEt_3) (Figure 1a), Ag(Piv) (Piv = 2, 2-dimethylpropionato), and Ag(Piv)(PEt_3) (Figure 1b) were synthesized in-house using literature methods.[15,11] For the β-diketonates, a reaction between Ag_2O and the β-diketone was used.[11] Silver pivalate Ag(Piv) was synthesized in aqueous solution by reacting $AgNO_3$ with KPiv.[15] Ag(Piv)(PEt_3) was synthesized simply by adding PEt_3 to AgPiv in toluene solution.[15] ^1H and ^{13}C NMR spectra were recorded with a Varian Mercury 300 MHz instrument at ambient temperature. Chemical shifts were referenced to $SiMe_4$ and are given in ppm. Thermogravimetric analysis (TGA) was performed with a Mettler Toledo Star^e system equipped with a TGA 850 thermobalance using a flowing nitrogen atmosphere at 1 atm. The heating rate was 10 °C/min, and the sample weight was 10−11 mg. TGA equipment recorded also single differential thermal analysis (SDTA) data.

Synthesis of Ag(fod). Ag_2O (0.29 g (1.24 mmol)) was weighed into a 50 mL Schlenk bottle. Ten milliliter of toluene and 0.74 g (2.48 mmol) of Hfod were added. While stirring, black Ag_2O disappeared and a clear solution resulted. Toluene and volatile impurities were evaporated away with the help of a vacuum and water bath. The product was a white powdery solid. Yield, 0.91 g (91%). ^1H NMR(C_6D_6 300 MHz) 1.13 (s, 18H, CH_3), 5.81 (s, 1H, CH), ^{13}C NMR (C_6D_6, 75 MHz): 28.56 ($C(CH_3)_3$), 43.22($C(CH_3)_3$), 85.01 (CH), 107.97 (CF_2), 114.97 (CF_2), 120.50 (CF_3), 174.27 (CO), 207.00 (CO).

Synthesis of Ag(fod)(PEt_3). Ag_2O (2.22 g (9.59 mmol)) was weighed into a 350 mL Schlenk bottle. One hundred milliliters of toluene and 5.69 g (19.19 mmol) of Hfod were added. To this solution, 22.70 g of 10% PEt_3 (2.27 g, 19.19 mmol) in hexane was added. During the addition of PEt_3, the black Ag_2O disappeared and a clear dark yellow solution resulted. Toluene and volatile impurities were evaporated away with the help of a vacuum. At first, the product was a yellowish liquid, but while standing, a colorless crystalline material formed. Yield 9.60 g (96%). ^1H NMR(C_6D_6, 300 MHz) 0.62−0.77 (m, 9H, CH_3), 0.81−0.94 (m, 6H, CH_2), 1.24 (s, 9H, CH_3), 6.17 (s, 1H, CH); ^{13}C NMR (C_6D_6, 75 MHz): 9.43 (CH_3), 9.50(CH_3), 17.73 (CH_2), 17.98 (CH_3), 28.65 ($C(CH_3)_3$), 43.04 ($C(CH_3)_3$), 90.45 (CH), 111.98 (CF_2), 117.08(CF_2), 121.35 (CF_3), 172.72 (CO), 205.70 (CO).

Synthesis of Ag(thd)(PEt_3). Ag_2O(0.28 g (1.22 mmol)) was weighed into a 50 mL Schlenk bottle. Ten milliliters of toluene and 0.45 g (2.44 mmol) of Hthd were added. To this solution, 2.89 g of 10% PEt_3 (0.289 g, 2.44 mmol) in hexane was added. During the addition of PEt_3, the black Ag_2O disappeared and a clear solution resulted. Toluene and volatile impurities were evaporated away with the help of a vacuum. At first, the product was a colorless liquid, but while standing, a colorless crystalline material formed. Yield, 0.95 g (95%). ^1H NMR(C_6D_6 300 MHz) 0.62−0.77 (m, 9H, CH_3), 0.81−0.94 (m, 6H, CH_2), 1.47 (s, 18H, CH_3), 5.99 (s, 1H, CH), ^{13}C NMR (C_6D_6, 75 MHz): 9.52 (CH_3), 9.59(CH_3), 17.92 (CH_2), 18.22 (CH_3), 29.77 ($C(CH_3)_3$), 42.59 ($C(CH_3)_3$), 88.54 (CH), 200.32 (CO).

Earlier unknown crystal structures of Ag(thd)(PEt_3) and Ag(fod)(PEt_3) were solved. Single crystals suitable for X-ray diffraction were obtained from the originally liquid synthesis products which crystallized slowly while standing at room temperature. The crystals were mounted on a glass fiber with the viscous oil-drop method.[17] The equipment used was a Bruker Nonius KappaCCD diffractometer (MoK_α, λ = 0.71073 Å). Area-detector scaling and absorption corrections were done with a program SADABS.[18] Structures were solved and refined with the SHELX97[19] software package. All non-hydrogen atoms were refined anisotropically; H atoms were calculated according to the ideal geometry. Table 1 presents the summary of crystal data, data collection, and refinement parameters. Illustrations were produced by the SHELXTL[20] program. CCDC reference numbers of Ag(thd)(PEt_3) and Ag(fod)(PEt_3) are 809279 and 809280, respectively.

Film Growth. Silver thin films were deposited in a Beneq TFS-200 ALD-reactor, capable of depositing on 200 mm wafers, with a remote plasma configuration (Figure 2). Plasma was generated with capacitive coupling with a 13.56 MHz rf power source. The plasma power was 100 W. The distance between the substrate and the grid, which was the bottom electrode, was 4 cm. Plasma activated hydrogen was used as the reducing agent. Hydrogen gas (99.999%, AGA) was mixed with argon (99.999%, AGA) to ensure plasma ignition. In general, the hydrogen flow was 20 sccm and the argon plasma gas flow 140 sccm. The hydrogen flow was not pulsed because no reaction between the precursor and molecular hydrogen was noticed at the applied growth temperatures. Argon carrier gas flow was typically 170 sccm. Gases were purified on-site before mixing with Aeronex GateKeeper and Entergris GateKeeper purifiers. To examine the effect of gas impurities on film composition, a few depositions were done without gas purifiers. Pressure in the reactor was around 5−8 mbar during depositions.

The precursor, Ag(fod)(PEt_3), was loaded onto an open boat and vaporized at 106 °C. The precursor was pulsed into the reaction chamber with inert gas valving. The substrates were soda lime glass (5 × 5 cm^2) and Si(100) wafer (150 mm, with a native oxide) loaded at the same time for each growth experiment. The metal precursor pulse length was varied between 1−4 s and the hydrogen plasma pulse between 3−5 s. Typically, the purge length after the metal precursor was 5 s and after the plasma exposure 3 s. The used growth temperatures were 120−150 and 200 °C.

Analysis of the Films. The thicknesses of the films deposited on Si(100)-substrates were measured with energy dispersive X-ray spectroscopy (EDS). EDS measurements were performed with an Oxford INCA 350 Energy spectrometer connected to a Hitachi S-4800 field

Table 1. Summary of Crystal Data, Data Collection, and Refinemental Parameters for $Ag(thd)(PEt_3)$ and $Ag(fod)(PEt_3)$

compound	$Ag(thd)(PEt_3)$	$Ag(fod)(PEt_3)$
empirical formula	$Ag_2O_4C_{34}H_{68}P_2$	$Ag_1O_3C_{16}H_{25}F_7P_1$
formula weight [g mol^{-1}]	818.56	521.20
temperature [K]	173(2)	123(2)
wavelength [Å]	0.71073 (Mo−Kα)	
crystal system	triclinic	orthorhombic
space group	*P* −*1* (no. 2)	*P b c n* (no. 60)
unit cell dimensions [Å], [deg]	*a* = 11.004(2)	*a* = 15.573(3)
	α = 81.67(3)	
	b = 13.139(3)	*b* = 16.835(3)
	β = 87.02(3)	
	c = 15.310(3)	*c* = 16.276(3)
	γ =69.85(3)	
volume [$Å^3$]	2056.1(7)	4267.1(15)
Z	2	8
density (calculated) [Mg m^{-3}]	1.322	1.623
absorption coefficient [mm^{-1}]	1.061	1.086
F(000)	856.0	2096
crystal size [mm^3]	0.04 × 0.10 × 0.20	0.03 × 0.20 × 0.34
theta range for data collection [deg]	5.00 to 27.50	5.00 to 27.50
index ranges	$-14 \le h \le 14$	$-20 \le h \le 20$
	$-17 \le k \le 17$	$-21 \le k \le 21$
	$-19 \le l \le 18$	$-20 \le l \le 21$
reflections collected	34597	69786
independent reflections	9345	4868
reflections with $I > 2\sigma(I)$	7516	3757
completeness to θ [deg]	27.50° = 99.2%	27.50° = 99.2%
refinement method	Full-matrix least-squares on F^2	
data/restraints/parameters	9345/0/379	4868/6/250
goodness-of-fit on F^2	0.770	1.146
R_{int}	0.0385	0.0755
R_1 indices [$I > 2\sigma(I)$][a]	0.0284	0.0747
wR_2 indicecs [$I > 2\sigma(I)$][b]	0.0898	0.1658
R_1 indices (all data)[a]	0.0445	0.0980
wR_2 indices (all data)[b]	0.1047	0.1826
largest difference hole and peak [e $Å^{-3}$]	−0.398 and 0.371	−1.071 and 1.667

[a] $R_1 = \Sigma||F_o| - |F_c||/|F_o|$. [b] $wR_2 = [\Sigma w(F_o^2 - F_c^2)^2/\Sigma w(F_o^2)^2]^{1/2}$.

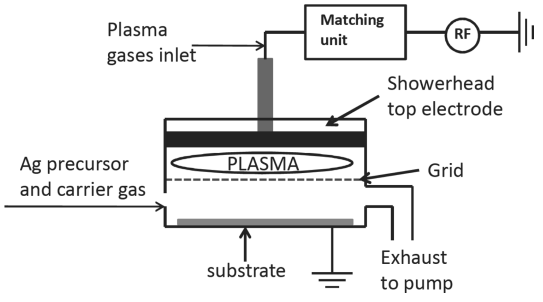

Figure 2. Schematic of the remote plasma configuration of the Beneq TFS-200 ALD-reactor.

emission scanning electron microscope (FESEM). The bulk density (10.5 g/cm^3) of silver was used to calculate the thicknesses from the *k* ratios measured for silver L_α lines.[21] The actual film thicknesses are probably somewhat higher than those calculated using the bulk density because the actual film densities are most likely lower than the bulk value. The morphologies of the films were studied with FESEM and atomic force microscopy (AFM) (Nanoscope V, Veeco Instruments). The crystal structure of the film was analyzed by X-ray diffraction (XRD) with a PANalytical ÝPert PRO MPD X-ray diffractometer. The measurements were performed in parallel beam geometry with copper K_α (λ = 1.5406 Å) radiation. Resistivities of the films were measured with a four-point probe (Keithley 2400 SourceMeter with a Cascade Microtech four-point probe). Compositions of selected silver films were analyzed with time-of-flight elastic recoil detection analysis (TOF-ERDA)[22] and Rutherford backscattering spectrometry (RBS). The TOF-ERDA and RBS measurements were performed at the University of Jyväskylä with 7.5 MeV $^{37}Cl^{4+}$ and 3 MeV $^4He^{1+}$ ions, respectively, as projectiles.

RESULTS AND DISCUSSION

Precursor Characterization. In the literature, there are many studies on different *β*-diketonates and carboxylates of silver with or without ancillary ligands as possible precursors for MOCVD.

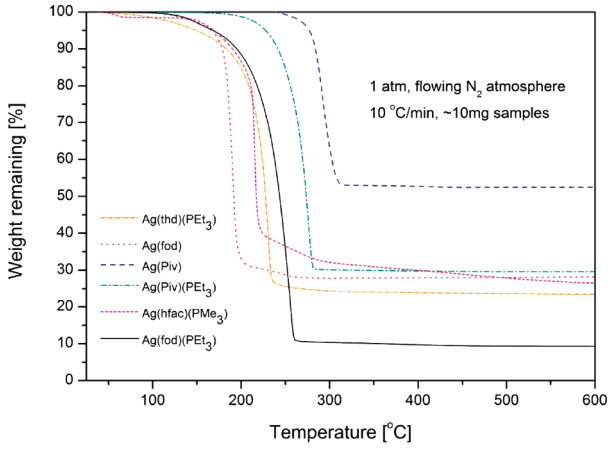

Figure 3. TGA curves of the considered Ag precursors. (thd = 2,2,6,6-tetramethyl-3,5-heptanedionato, piv = 2,2-dimethylpropionato, and hfac =1,1,1,5,5-hexafluoroacetylacetonato.)

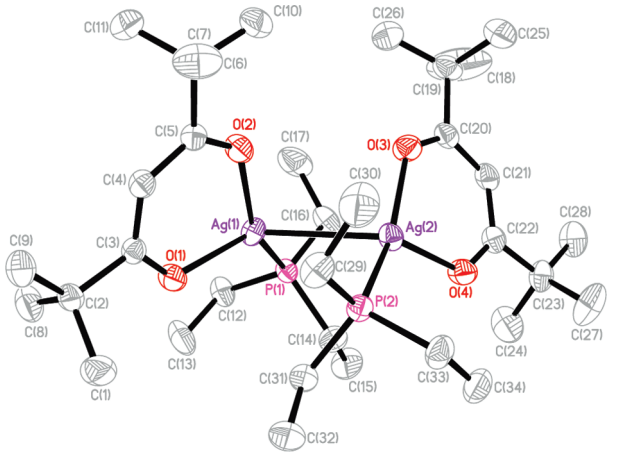

Figure 4. Molecular structure of $[Ag(thd)(PEt_3)]_2$. Asymmetric unit. Hydrogen atoms are omitted for clarity, and thermal ellipsoids are on a 50% level.

In most cases, the available normal atmospheric pressure TGA studies reveal that the compounds decompose and leave residues approximately equal to or larger than the amount of silver in the compounds.[23,24] However, there are some exceptions: Ag(thd)-(P^nBu_3) (Ag-content = 22%) has been reported to leave 11% residue,[24] Ag(fod)(PMe_3) (Ag-content = 22.5%) and Ag(fod)-(PEt_3) (Ag-content =20.7%) left, respectively, only 4% and 1% residues,[11] and Ag(hfac)(C≡NMe) (Ag-content =30.3%) was reported to leave a residue of 8%.[25] In the present study, atmospheric pressure thermogravimetric analysis was performed on several silver precursors with β-diketonato or carboxylato ligands (Figure 3).

On the basis of TGA, Ag(fod)(PEt_3) was found as the best choice for the ALD process. In our studies, all the other Ag compounds except Ag(fod)(PEt_3) left residues that were larger or approximately equal to the theoretical amount of silver in the compounds which implies that they decomposed without any evaporation of the intact compound. Ag(fod)(PEt_3) left only 6% residue though the Ag content is 22.7%, which proves that a large part of the compound Ag(fod)(PEt_3) itself evaporates. Weight loss of Ag(fod)(PEt_3) begins around 110 °C and is complete at approximately 270 °C. The weight loss is half complete at 240 °C. SDTA (not shown) showed an endotherm due to evaporation which is in contrast with all the other β-diketonates studied, which show a strong exotherm at the temperature of the weight loss. The TGA of Ag(fod)(PEt_3) lets us suggest that this liquid would be thermally stable at least up to 230 °C. However, silver thin films could not be deposited at such high temperatures. It is known that the stability of a compound as a liquid may be different compared with the stability in gas phase and that adsorbed on a surface.

The synthesis method employed for Ag(fod)(PEt_3) uses the well-known very simple reaction among Ag_2O, β-diketone, and an ancillary ligand. Pure Ag(fod)(PEt_3) is an easily handled yellowish solid at room temperature which turns into liquid at 25 °C.

Earlier unknown structures of two Ag-compounds were solved. The structure of Ag(thd)(PEt_3) is dimeric (Figure 4). There is a weak interaction between the silver atoms. The Ag1 to Ag2 distance is 2.948(1) Å, while in metallic silver, the atomic separation is 2.89 Å. Other interactions between the monomeric units are absent. If the Ag to Ag interaction is not taken into account, the coordination sphere of the Ag atoms may be described as distorted trigonal planar, otherwise, with Ag to Ag interactions, distorted tetragonal. In Ag to O distances, there is a slight difference between the two oxygen atoms of the β-diketonato ligands. The Ag1 to O1 distance is 2.272(2) Å, while the Ag1 to O2 distance is 2.200(2) Å. The Ag2 to O3 distance is 2.175(2) and Ag2 to O4 2.312(2) Å. However, in the C−O bond distances there are no significant differences (1.252(3)−1.262(3) Å), and also the bond distances between the carbon atoms in the chelate rings are approximately equal (1.398(4)−1.408(4) Å), which indicates that the charges of the thd ligands are well delocalized. The Ag to P bond distances are 2.322(1) and 2.331(1) Å. These values are in line with those found in the literature.

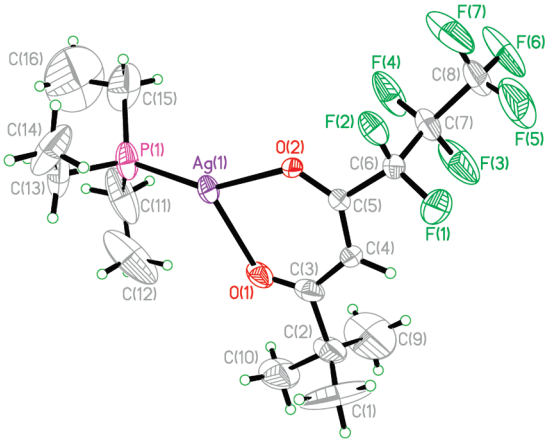

Figure 5. Asymmetric unit of $[Ag(fod)(PEt_3)]_2$ and molecular structure of Ag(fod)(PEt_3). Hydrogen atoms are omitted for clarity, and thermal ellipsoids are on a 50% level.

The structure of Ag(fod)(PEt_3) is also dimeric. However, interactions between the monomeric units are completely different. Figure 5 shows the asymmetric unit which is a monomeric molecule. Figure 6 shows the dimers formed in the structure. There is no interaction between the Ag atoms, and the Ag to Ag distance is 3.490 Å. Instead, the β-diketonato ligands which are chelated to one Ag atom also share one oxygen atom with the

dx.doi.org/10.1021/cm200402j |Chem. Mater. 2011, 23, 2901–2907

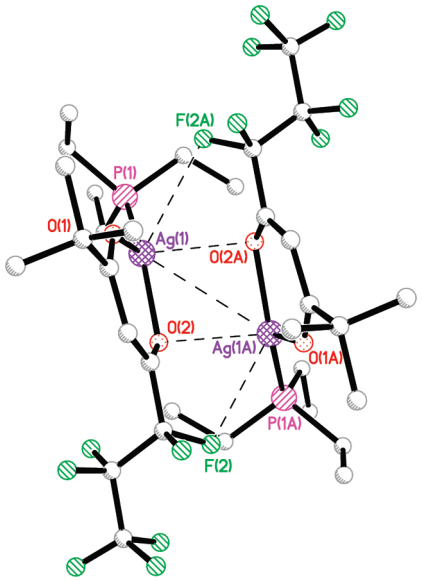

Figure 6. Molecular structure of $[Ag(fod)(PEt_3)]_2$ showing the dimers in the crystal. For clarity, hydrogen atoms are omitted, and other atoms are drawn isotropic at a 20% probability level.

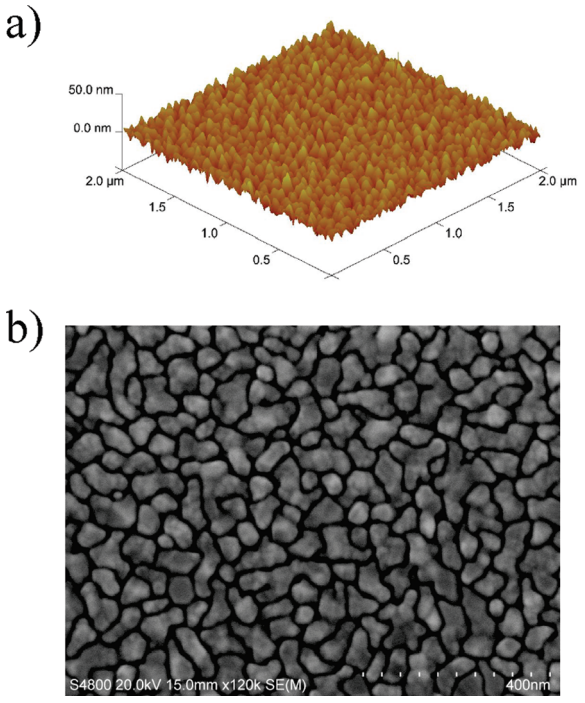

Figure 7. (a) $2 \times 2\ \mu m^2$ AFM image of a 17 nm thick Ag film deposited at 120 °C. Height scale: 50 nm. (b) SEM image of the same film.

second Ag atom. The bridging O atom is on the side of the C_3F_7-chain of the fod ligand. The bond distance between the terminal oxygen atom (O1) and Ag1 is 2.319(5) Å. O2 is 2.231(4) Å from Ag1 and 2.684 Å from Ag1A (Figure 6). There is also interaction between the F2A and Ag1. The distance between these atoms is 3.111 Å. Despite this interaction, this compound is thermally quite stable, and also, there does not seem to be any substantial fluorine contamination in the films deposited using this precursor. The Ag to P distance is 2.326(2) Å, which is quite typical. One

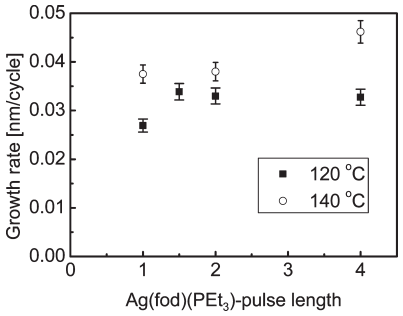

Figure 8. Growth rate of Ag thin films at different substrate temperatures as a function of a $Ag(fod)(PEt_3)$-pulse length. The plasma pulse length was 5 s. Error bars refer to the estimated error of EDS quantification.

could speculate that the interaction between the silver atoms in the precursor, like in $Ag(thd)(PEt_3)$, is not beneficial for the thermal stability.

Film Deposition. Silver films were successfully deposited on silicon and glass substrates using $Ag(fod)(PEt_3)$ as a metal precursor. Visually, the films appeared mirror-like. The film growth started with the formation of nanoclusters during the first cycles and further on resulted in a continuous film. Films that were thinner than 10 nm were noncontinuous according to the SEM images. After the formation of a continuous layer, the film continued to grow onto itself, and roughness increase was moderate. For example, a 17 nm thick Ag film deposited at 120 °C had a rms-roughness of 4.8 nm (Figure 7a), while a 30 nm film resulted in a rms-roughness of 5.4 nm. Figure 7b shows a SEM image of a 17 nm thick film. The film is seen to consist of large grains with a size of about 40−90 nm.

The ALD-type saturative growth was achieved at deposition temperatures of 120−140 °C (Figure 8). At 120 °C, the growth rate was 0.03 nm per cycle. At higher temperatures, the growth rate increased to some extent (0.038 nm/cycle). The effect was more obvious with longer $Ag(fod)(PEt_3)$ pulses. In addition, at temperatures exceeding 140 °C the thickness nonuniformity increased, being indicative of thermal decomposition of the precursor. It should be pointed out that during the depositions the temperature of the reaction chamber wall increased roughly 6−8 °C when the plasma power was 100 W. If the metal precursor pulse length was not long enough, the film grew only on the inlet side of the substrate. Still, the growth was saturated and film thickness controllable. A 4 s pulse length was necessary to obtain almost uniform growth across the whole substrate area of 200 mm diameter when the carrier gas flow was 170 sccm. In every film, some nonuniformity was noticed, especially in the inlet region. Nonuniformity can also be a sign of weak precursor decomposition. However, it is believed that optimization of the carrier gas flow will diminish the nonuniformity.

The plasma exposure time was varied between 3−5 s. With the shortest exposure time, the growth rate was lower (0.027 nm/cycle) over the whole deposition zone. To keep the total cycle time at a reasonable level, 5 s was decided to be the maximum plasma exposure time used in the growth experiments.

The saturated growth rate is quite low compared to that in the previously published ALD process of silver. With $Ag(Piv)(PEt_3)$, the growth rate was 0.12 nm per cycle.[15] In the current study, the lower growth rate may be explained by the bulkiness of the fod-ligand. The bulky ligand causes steric hindrance in the

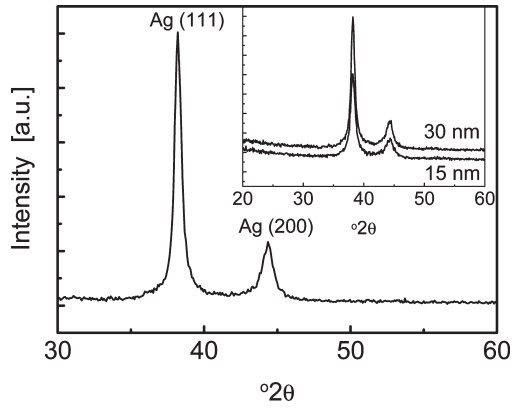

Figure 9. XRD pattern of a 17 nm thick silver film deposited on silicon (100) substrate. The inset shows the effect of film thickness on an XRD pattern. All of the films were deposited at 120 °C.

chemisorption layer and thereby lowers the growth rate. However, the bulkiness of the fod ligand can prevent the precursor from decomposition.

Properties of the Films. The adhesion of a silver film to the silicon substrate was evaluated by the Scotch tape test. Typically, the films which were 30 nm or thinner passed the test. The thicker films were not systematically tested. Even if passing the tape test, all the films could easily be damaged by scratching with gloves or tweezers.

All the films deposited were polycrystalline. The (111) and (200) reflections of cubic Ag structure were identified (Figure 9). The (111) reflection was the strongest one. As expected, the intensity of the reflections increased with increasing Ag film thickness, but the intensity ratio remained the same.

The resistivities were measured from the films deposited on glass. There was quite a lot of scatter in the results. Very thin films had high resistivities, but, for example, already 22 nm thick films exhibited resistivities of 6−8 $\mu\Omega\cdot$cm. The results can be compared with the resistivities of the evaporated polycrystalline silver thin films.[8] An evaporated 23 nm thick film had the resistivity of roughly 3.5 $\mu\Omega\cdot$cm. Compared to this, the resistivities achieved in the present study are encouraging especially because it is known that chemically deposited films usually have higher quantities of impurities leading to higher resistivities than the physically deposited thin films. In the previously published ALD study on silver, the resistivity of a 40 nm thick film was 6 $\mu\Omega\cdot$cm.[15] The resistivities achieved in the CVD processes of silver with Ag(fod)(PEt_3) as a precursor have typically been in the range of 1.9−3 $\mu\Omega\cdot$cm, but in those studies, the films were much thicker than those here.[11,13,14] CVD silver films obtained from (1,5-cyclooctadiene)(1,1,1,5,5,5-hexafluoroacetylacetonato) silver(I) (Ag(hfac)COD) had a resistivity of about 6 $\mu\Omega\cdot$cm at a thickness of 50 nm.[26]

A 17 nm thick film deposited at 120 °C without gas purifiers contained about 85 at.% silver, 7 at.% hydrogen, 3 at.% carbon, 3 at.% oxygen, 0.9 at.% phosphorus, 0.5 at.% fluorine, and 0.7 at.% nitrogen as analyzed by TOF-ERDA from the near-surface region of the film. The content of fluorine was also analyzed by RBS to get a better estimation of the real content. The composition of a silver film deposited with gas purifiers was also analyzed: no significant difference in elemental contents was noticed compared to that in the film deposited without purifiers. The impurities are most likely residues from incomplete reactions. It is also noticeable that the F contamination is low, though the precursor contains fluorine and there is even an Ag to F interaction in the solid phase (Figure 6). Some oxygen and carbon impurities may be a consequence of contamination after deposition since the TOF-ERDA measurements were performed after long air exposure. However, the occurrence of nitrogen in the film was unexpected because no nitrogen compounds were used in any stage of the precursor synthesis or deposition. The high surface roughness with respect to the film thickness spreads the elemental distributions in the TOF-ERDA measurement. Therefore, depth profiles can show higher than true contents for elements that are located at the film surface and interface. The given impurity contents can be considered as the upper limit for H, C, O, P, F, and N.

Overall, the films deposited with the present process contained less impurities than the films deposited with the previously presented Ag-process.[15] The film compositions are quite similar with some exceptions. In the present study, no silicon was detected, although the measurement was performed on the film deposited on silicon, meaning that the film completely covered the silicon substrate which was also obvious from the SEM image (Figure 7). The present film contained more carbon, most likely because of the higher amount of carbon atoms in the Ag(fod)-(PEt_3)-molecule compared to that in Ag(Piv)(PEt_3).

CONCLUSIONS

For the first time, silver thin films were successfully deposited on 200 mm wafer sizes with PEALD. Ag(fod)(PEt_3) and plasma activated hydrogen were used as the precursors. The thermal properties of the other silver compounds known in the literature were also studied, but Ag(fod)(PEt_3) was found out to be the most suitable precursor for PEALD.

The process temperature range was relatively narrow, but the ALD-type saturative growth was achieved at 120−140 °C. The films contained 85 at.% of silver. The main impurities were hydrogen, carbon, and oxygen. The impurities affected the electrical properties, but still relatively low resistivity values of 6−8 $\mu\Omega\cdot$cm were achieved.

The aim of the research was to introduce a new ALD process for Ag thin films on large area substrates. However, several plasma related parameters were not investigated in detail, and the work is to be continued.

ASSOCIATED CONTENT

Supporting Information. Crystallographic information files (CIF) for compounds Ag(thd)(PEt_3) and Ag(fod)(PEt_3) as electronic copies (CIF and PDF). This material is available free of charge via the Internet at http://pubs.acs.org.

AUTHOR INFORMATION

Corresponding Author
*E-mail: maarit.kariniemi@helsinki.fi.

ACKNOWLEDGMENT

Dr. Esa Puukilainen is thanked for technical support during AFM measurements. The study was partially supported by the Academy of Finland (Project No. 128805) and Finnish Centre of Excellence Programme 200620100 (Project No. 213503, Nuclear and Accelerator Physics Programme at JYFL).

REFERENCES

(1) Ritala, M.; Niinistö, J. In *Chemical Vapour Deposition: Precursors, Processes and Applications*; Royal Society of Chemistry: Cambridge, UK, 2008; pp 158−206.
(2) George, S. M. *Chem. Rev.* **2010**, *110*, 111–131.
(3) Ozbay, E. *Science* **2006**, *311*, 189.
(4) Barnes, W. L.; Dereux, L.; Ebbesen, T. W. *Nature* **2003**, *424*, 824.
(5) International Technology Roadmap for Semiconductors. [Online] 2009; http://www.itrs.net/Links/2009ITRS/Home2009.htm.
(6) Piedade, A. P.; Vieira, M. T.; Martins, A.; Silva, F. *Nanotechnology* **2007**, *18*, 105103.
(7) Im, H.; Lindquist, N. C.; Lesuffleur, A.; Oh, S.-H. *ACS Nano* **2010**, *4*, 947.
(8) De Vries, J. W. C. *Thin Solid Films* **1988**, *167*, 25.
(9) Liu, H.; Wang, B.; Leong, E. S. P.; Yang, P.; Zong, Y.; Si, G.; teng, G.; Teng, J.; Maier, S. A. *ACS Nano* **2010**, *4*, 3139.
(10) Kapaklis, V.; Poulopoulos, P.; Karoutsos, V.; Manouras, Th.; Politis, C. *Thin Solid Films* **2006**, *510*, 138.
(11) Yuan, Z.; Dryden, N. H.; Vittal, J. J.; Puddephatt, R. J. *Chem. Vap. Deposition* **1995**, *7*, 1696.
(12) Serghini-Monim, S.; Yuan, Z.; Griffiths, K.; Norton, P. R.; Puddephatt, R. J. *J. Phys. Chem.* **1995**, *99*, 9230.
(13) Gao, L.; Härter, P.; Linsmeier, Ch.; Gstöttner, J.; Emling, R.; Schmitt-Landsiedel, D. *Mater. Sci. Semicond. Process* **2004**, *7*, 331.
(14) Gao, L.; Härter, P.; Linsmeier, Ch.; Wiltner, A.; Emling, R.; Schmitt-Landsiedel, D. *Microelectron. Eng.* **2005**, *82*, 296.
(15) Niskanen, A.; Hatanpää, T.; Arstila, K.; Leskelä, M.; Ritala, M. *Chem. Vap. Deposition* **2007**, *1*, 408.
(16) Chalker, P. R.; Romani, S.; Marshall, P. A.; Rosseinsky, M. J.; Rushworth, S.; Williams, P. A. *Nanotechnology* **2010**, *21*, 405602.
(17) Kottke, T.; Stalke, D. *J. Appl. Crystallogr.* **1993**, *26*, 615.
(18) Sheldrick, G. M. *SADABS, a Software for Empirical Absorption Correction*; University of Gottingen: Gottingen, Germany, 2000.
(19) Sheldrick, G. M. *Acta Crystallogr., Sect. A.* **2008**, *64*, 112.
(20) *SHELXTL Reference Manual*, version 5.1; Bruker AXS, Analytical Instrumentation: Madison, WI, 2000.
(21) Waldo, R. A. *Microbeam Anal.* **1988**, 310.
(22) Putkonen, M.; Sajavaara, T.; Niinistö, L.; Keinonen, J. *Anal. Bioanal. Chem.* **2005**, *382*, 1791.
(23) (a) Szlyk, E.; Szczesny, R.; Wojtczak, A. *Dalton. Trans.* **2010**, *39*, 1823. (b) Edvards, D. A.; Mahon, M. F.; Molloy, K. C.; Ogrodnik, V. *J. Mater. Chem.* **2003**, *13*, 563. (c) Zanotto, L.; Benetollo, F.; Natali, M.; Rossetto, G.; Zanella, P.; Kaciulis, S.; Mezzi, A. *Chem. Vap. Deposition* **2004**, *10*, 207. (d) Darr, J. A.; Poliakoff, M.; Blake, A. J.; Li, W.-S. *Inorg. Chem.* **1998**, *37*, 5491. (e) Fragalà, E. M.; Malandrino, G.; Puglisi, O.; Benelli, C. *Chem. Mater.* **2000**, *12*, 290.
(24) Ngo, S. C.; Banger, K. K.; Toscano, P. J.; Welch, J. T. *Polyhedron* **2002**, *21*, 1289.
(25) Yuan, Z.; Dryden, N. H.; Li, X.; Vittal, J. J.; Puddephatt, R. J. *J. Mater. Chem.* **1995**, *5*, 303.
(26) Bahlawane, N.; Premkumar, P. A.; Brechling, A.; Reiss, G.; Kohse-Höinghaus, K. *Chem. Vap. Deposition* **2007**, *13*, 401.